Homogeneity and Isotropy Restoration (HIRE)-Theoretic Multigroup Neutron Transport Equations and Two-Level p-CMFD Acceleration Scheme

Nam Zin Cho
Korea Advanced Institute of Science and Technology
291 Daehak-ro, Yuseong-gu, Daejeon, Korea 34141
nzcho@kaist.ac.kr

Abstract: This paper presents a novel approach to derive multigroup neutron transport equations from the continuous-energy transport equation while achieving group-wise condensation equivalence. The Homogeneity and Isotropy Restoration (HIRE) theory eliminates angle dependency in the group condensed total cross section, restoring material region homogeneity. Furthermore, it retains only the isotropic scattering cross section, eliminating the need for higher-order moment scattering cross sections. In order to preserve the reaction rate, we introduce the Partial Current Discontinuity Factor (PCDF). To address memory and computing time constraints in continuous-energy Monte Carlo whole-core simulations, we propose a two-step process: (i) analyze local problems with non-reflective boundary conditions using continuous-energy Monte Carlo simulations and transform them into the HIRE-based multigroup transport equations, and (ii) solve the global multigroup transport equations using deterministic methods like the discrete ordinates method or the method of characteristics, with acceleration schemes such as the unconditionally stable p-CMFD method, that is instrumental in a two-level W-cycle scheme.

1. Introduction

The first part of the paper revisits the derivation of the homogeneity and isotropy restoration (HIRE)-theoretic multigroup neutron transport equations [1], and the second part describes the two-level p-CMFD acceleration scheme for its iterative solution, with a discussion of the benefits in the use of partial currents [2].

Starting with the following neutron transport equation (in continuous energy),

$$\vec{\Omega}\cdot\nabla\varphi(\vec{r},E,\vec{\Omega})+\sigma_t(\vec{r},E)\varphi(\vec{r},E,\vec{\Omega})=\int d\Omega'\int dE'\sigma_s(\vec{r},E'\to E,\vec{\Omega}'\to\vec{\Omega})\varphi(\vec{r},E',\vec{\Omega}')$$
$$+\frac{\chi(E)}{k_{eff}}\int d\Omega'\int dE'\nu\sigma_f(\vec{r},E')\varphi(\vec{r},E',\vec{\Omega}')\,, \qquad (1)$$

the multigroup transport equations are written as

$$\vec{\Omega}\cdot\nabla\varphi_g(\vec{r},\vec{\Omega})+\sigma_{t,g}(\vec{r},\vec{\Omega})\varphi_g(\vec{r},\vec{\Omega})=\sum_{g'=1}^{G}\int d\Omega'\sigma_{s,gg'}(\vec{r},\vec{\Omega}'\to\vec{\Omega})\varphi_{g'}(\vec{r},\vec{\Omega}')$$
$$+\frac{\chi_g}{k_{eff}}\sum_{g'=1}^{G}\nu\sigma_{f,g'}(\vec{r})\phi_{g'}(\vec{r})\,, \qquad (2)$$

with standard notations.

In particular, the multigroup total cross section $\sigma_{t,g}$ defined as

$$\sigma_{t,g}(\vec{r},\vec{\Omega}) = \frac{\int_{E_g}^{E_{g-1}} dE\,\sigma_t(\vec{r},E)\varphi(\vec{r},E,\vec{\Omega})}{\int_{E_g}^{E_{g-1}} dE\,\varphi(\vec{r},E,\vec{\Omega})}, \tag{3}$$

is, traditionally, written and evaluated as, for material region *m*,

$$\sigma_{t,g}^{m} = \frac{\int_{\vec{r}\in V_m} dV \int d\Omega \int_{E_g}^{E_{g-1}} dE\,\sigma_t(\vec{r},E)\varphi(\vec{r},E,\vec{\Omega})}{\int_{\vec{r}\in V_m} dV \int d\Omega \int_{E_g}^{E_{g-1}} dE\,\varphi(\vec{r},E,\vec{\Omega})}, \tag{4}$$

in addition, removing the angular dependency in Eq. (3).

In this paper, as in Refs. [5–12], $\sigma_{t,g}$ is evaluated as defined in Eq. (4), but with partial current discontinuity factors (PCDFs) imposed at the material interface.

In the neutron transport calculation, the coarse mesh based acceleration methods [1–9] are widely used, because they are easily applied to the original transport calculation with various geometries. However, they exhibit slow convergence or divergent behavior (in some of the methods) for optically thick coarse mesh cells. This drawback limits the size of coarse mesh cells, incurring significant computational burden per iteration.

The present paper revisits the partial current-based coarse mesh finite difference (p-CMFD) acceleration method [5–8], that is unconditionally stable and more stable than other coarse mesh based acceleration methods. A recent extension with a two-level (two-grid) convergence speedup scheme [10–12] is shown to be very effective and made more efficient in this paper by using the Krylov subspace method first tested in a conference paper [13]. Numerical results of its application to the standard OECD benchmark problem and an enlarged problem show that the two-level scheme wrapped around by the Krylov subspace enhances the convergence rate of p-CMFD significantly, especially for optically thick coarse mesh cells (of fuel assembly size). The paper also suggests a super hexagonal geometry representation for fast reactor analysis in a two-level acceleration scheme.

2. Coarse Mesh Based Acceleration Methods and Limitations

Coarse mesh based acceleration methods usually consist of two parts: a high-order calculation and a low-order calculation. The high-order calculation employs transport methods (usually based on the discrete ordinates method or the method of characteristics in multigroup transport equations) with fixed fission source. The low-order calculation uses the balance equation, in which the high-order calculation provides parameters over each coarse mesh cell. The low-order calculation gives

the multiplication factor and the coarse mesh cell averaged scalar fluxes. The coarse mesh cell averaged scalar fluxes are then "modulated" or prolongated to be used in the fission source of the high-order equation for the next iteration.

To study the efficiency of an acceleration method, Fourier convergence analysis was performed on coarse mesh rebalance (CMR) [3,8], coarse mesh finite difference (CMFD) [8], and partial current based CMFD (p-CMFD) [5–8, 10]. The results in Figure 1 show that p-CMFD is always stable and more stable than the other methods. CMR shows divergent behavior for optically thin coarse mesh cells. CMFD and p-CMFD are very efficient for optically thin coarse mesh cells but not efficient for optically thick coarse mesh cells. (CMFD even diverges for optically thick coarse mesh cells, if $\widetilde{D}$ is used from the standard diffusion theory ($\widetilde{D}= 1/3\Sigma_t$). Note that a recent work on CMFD with linearly interpolating prolongation lp-CMFD [14] stabilizes this divergence).

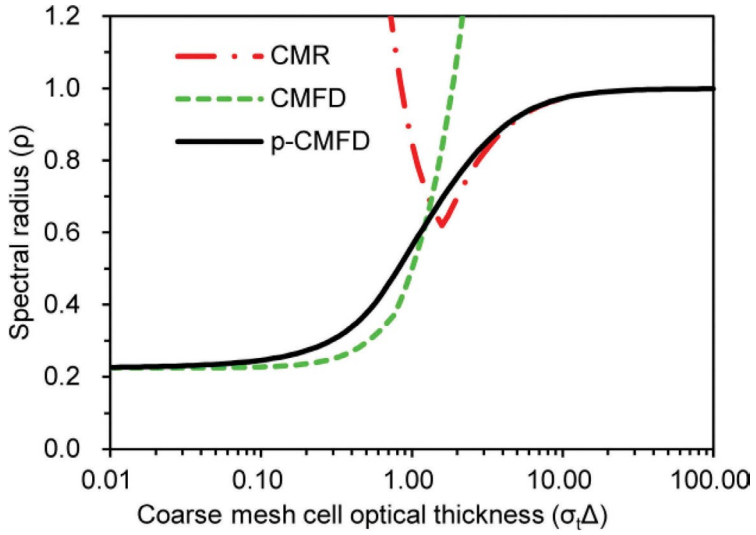

Figure 1. Spectral radii of CMR, CMFD, and p-CMFD.

Ref. 15 adjusted the diffusion coefficient in CMFD to improve the convergence rate (optimized). Similarly, the diffusion coefficient in p-CMFD can be also adjusted to optimize the spectral radius. Figure 2 shows the results in comparison. Even with the optimized diffusion coefficient, CMFD and p-CMFD show slow convergence in optically thick coarse mesh cells. This is a common property for all coarse mesh based acceleration methods; see Ref. 15 for CMFD, Ref. 10 for p-CMFD, and Ref. 14 for lp-CMFD. Therefore, the need arises to improve convergence for thick coarse mesh cells.

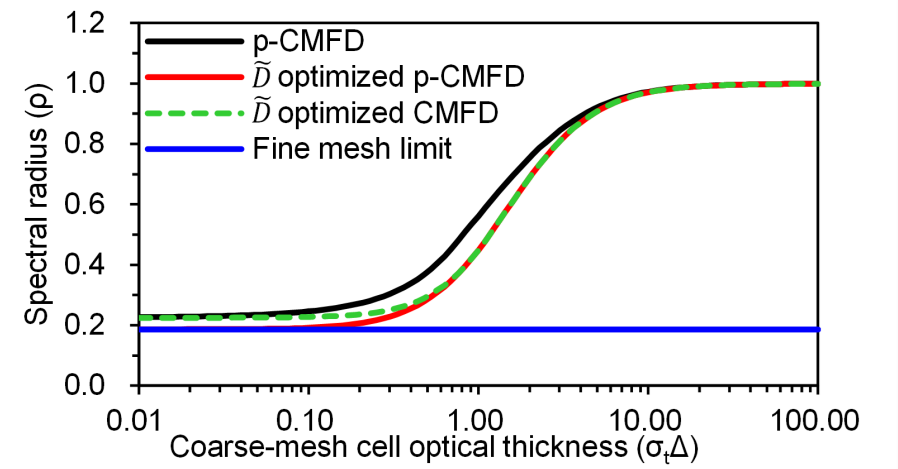

Figure 2. Spectral radii of the optimized CMFD and p-CMFD and the fine mesh limit.

3. Two-Level p-CMFD Acceleration

W-Cycle Scheme

The p-CMFD acceleration is a modification of the CMFD acceleration, in that p-CMFD is based on the use of partial currents (instead of net currents used in CMFD), resulting in:

i) p-CMFD is unconditionally stable,
ii) p-CMFD provides additional information, that is, transport partial currents on the interface of two coarse mesh cells, and thus,
iii) the incoming partial current allows a fixed-source problem formulation for a coarse mesh cell, whose solution provides in turn improved flux distribution and outgoing partial current (to the neighboring coarse mesh cell).

Note that CMFD [4] uses one correction coefficient to preserve the surface net current. On the other hand, p-CMFD uses two correction coefficients to preserve the two surface partial currents, respectively. (The surface net current is automatically preserved by the two surface partial currents.) In p-CMFD, there is little incentive to deal with the optimized diffusion coefficient (the improvement is only marginal in thin coarse mesh cells, where it is already very fast), instead we focus on thick coarse mesh cells, utilizing transport partial currents (see Figure 2). This section describes a two-level spatial coarse grid p-CMFD technique to speedup p-CMFD acceleration, particularly in optically thick coarse mesh cells. To reduce the spectral radius further, we also introduce a global/local iterative procedure to the low-level calculation in the two-level p-CMFD, as shown in the multi-grid literature notation in Figure 3. In Figure 3, a quarter pin forms an intermediate-mesh cell in p-IMFD and each assembly forms a coarse-mesh cell in p-CMFD (in light water reactors as in Numerical Results). Note that the p-IMFD rebalance calculations are used in restriction and prolongation for the scalar flux and partial currents.

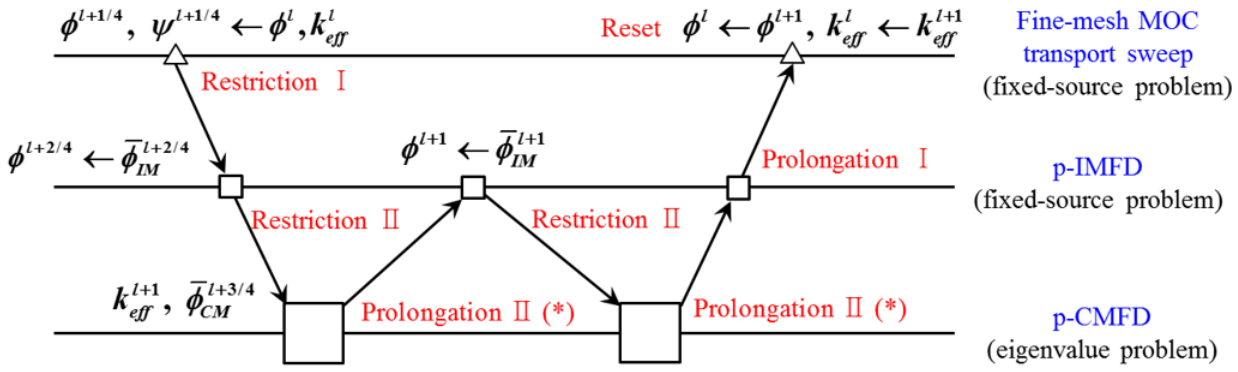

Figure 3. Two-grid representation of the p-CMFD computational flow for N =2 in W-cycle. (*with updated transport incoming partial currents)

Figure 4 is the convergence result of global/local iterations in the two-level p-CMFD acceleration for a 1-D version OECD/NEA benchmark problem. As the number of global/local iterations increases (N goes large), the spectral radius for optically thick coarse mesh cells reduces drastically, approaching that of the fine mesh limit in Figure 2.

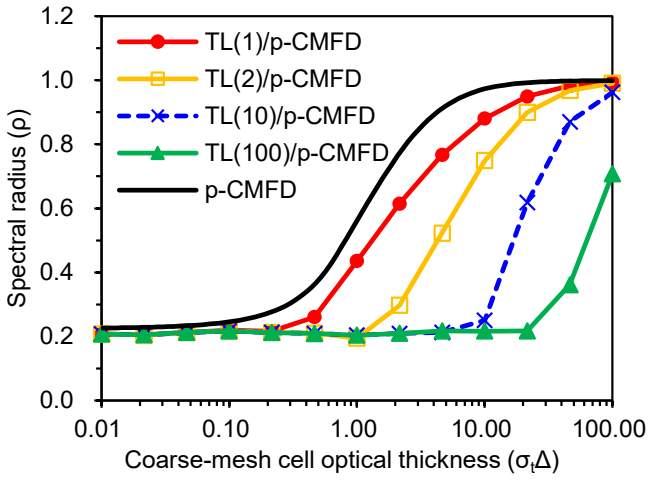

Figure 4. Spectral radius of global/local iteration in the two-level p-CMFD acceleration (TL(N)/p-CMFD: two-level p-CMFD with N global/local iterations).

Krylov Solution Algorithms

In the W-cycle scheme in Figure 3, Restriction I results in p-IMFD of intermediate-mesh cells and leads to the form,

$$\mathbf{A}\phi = \mathbf{b}, \tag{5}$$

that is a very large problem. It is then followed by the p-CMFD eigenvalue problem in coarse-mesh cells of the form,

$$\mathbf{M}\phi = 1/k_{eff}\mathbf{F}\phi \ . \tag{6}$$

They are both whole-core problems. Eq. (5) is solved by the the BiCGSTAB algorithm [16] and Eq. (6) by the Jacobian-Free Newton-Krylov (JFNK) algorithm [17]. In Eq. (6), ϕ and k_{eff} are considered as unknowns simultaneously, rendering them as roots of a nonlinear equation system. They are compared to the traditional methods of Gauss-Seidel (G-S) and power iteration (PI), respectively.

4. Numerical Results

The two-level p-CMFD is tested on a two-dimensional problem with seven-group cross section data that are specified in the OECD/NEA C5G7 benchmark report [18], and is shown in Figure 5.

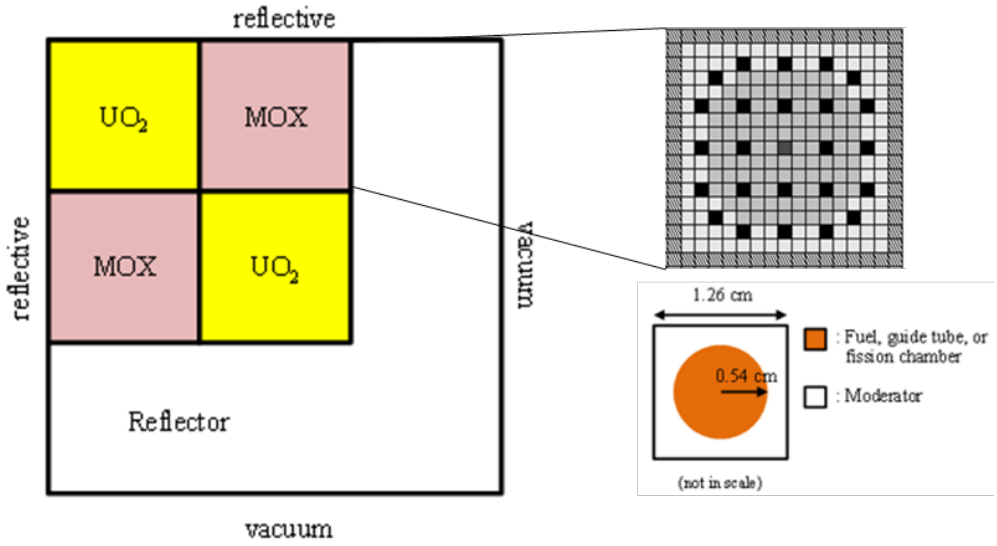

Figure 5. Geometry of OECD/NEA C5G7 benchmark problem.

The computational conditions are as follows: The method of characteristics (MOC) is used, with 40 mesh cells (5 ring divisions and 8 azimuthal sector divisions) per fuel pin cell and 64 mesh cells (8 by 8 rectangular mesh cells) per reflector (pseudo) pin cell. An intermediate-mesh cell is a quarter of a fuel pin or a reflector pin. Table I shows the various results in comparison. Note that the number of transport sweeps (that is most time-consuming among the various phases of the computation) reduces significantly from No Acceleration to p-CMFD, and more significantly to TL(*N*)/p-CMFD, as N increases. This effect outweighs well enough the increase in the number of p-CMFD power (or JFNK) iterations. Additional results on an enlarged OECD/NEA C5G7 benchmark problem are available in a github addendum [19] and reproduced here in Figure 6 and Table II. As expected, the speedup becomes larger as the problem becomes larger.

Table I. Results of OECD/NEA 2-D C5G7 (3 by 3) Benchmark Problem

Methods	No Acc.	p-CMFD	TL(1)/p-CMFD			TL(4)/p-CMFD		
	*a**	*a**	*a**	*b**	*c**	*a**	*b**	*c**
k_{eff}	1.18658	1.18658	1.18658	1.18658	1.18658	1.18658	1.18658	1.18658
Number of transport sweep iterations	1017	473	28	28	27	18	18	18
Number of p-CMFD Power (or JFNK) Iterations	0	4316	436	436	217	723	723	386
Transport sweep calculation time (sec) †	3148.618	1468.528	87.509	86.188	82.766	55.467	56.747	56.993
Whole-core p-IMFD time (sec)	0	0	5.311	3.034	2.06	2.8	1.859	1.376
Local p-IMFD time (sec)	0	0	4.558	2.834	2.162	8.819	6.602	4.859
Whole-core p-CMFD time (sec)	0	15.802	0.937	0.925	0.944	2.368	2.379	2.581
Total calculation time (sec)	3149.01	1484.67	98.412	93.081	88.017	69.552	67.687	65.9
Speedup	1	2.12	32.00	33.83	35.78	45.28	46.52	47.78
Percentage of transport sweep time in total calculation time	99.99	98.91	88.92	92.59	94.03	79.75	83.84	86.48

a: Gauss-Seidel +Power Iteration, b*: BiCGSTAB +Power Iteration, c*: BiCGSTAB +JFNK*
† : a single thread of a CPU (Intel i7-7700K)

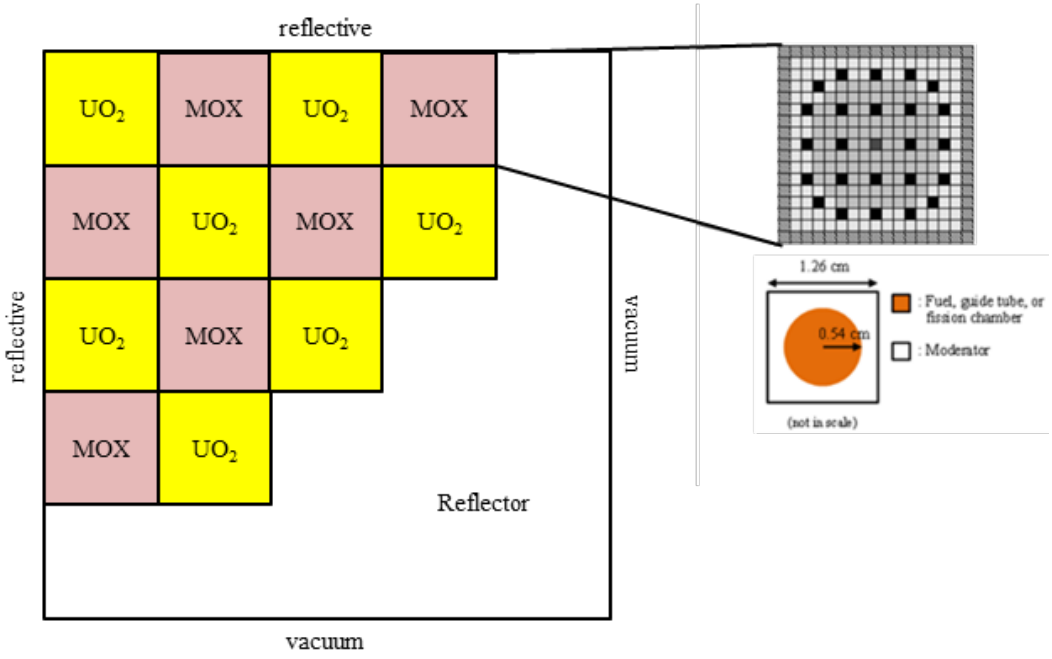

Figure 6. Geometry of enlarged C5G7 benchmark problem.

Table II. Results of Enlarged 2-D C5G7 (5 by 5) Benchmark Problem

Methods	No Acc.	p-CMFD	TL(1)/p-CMFD			TL(4)/p-CMFD		
	*a**	*a**	*a**	*b**	*c**	*a**	*b**	*c**
k_{eff}	1.23141	1.23141	1.23141	1.23141	1.23141	1.23141	1.23141	1.23141
Number of transport sweep iterations	2241	438	48	48	49	18	18	18
Number of p-CMFD Power (or JFNK) Iterations	0	4584	895	893	646	1023	1023	742
Transport sweep calculation time (sec) †	19874.194	3852.734	424.896	433.586	432.902	159.347	159.241	158.804
Whole-core p-IMFD time (sec)	0	0	23.143	13.831	8.467	8.203	5.515	3.536
Local p-IMFD time (sec)	0	0	19.212	12.682	9.307	25.41	18.688	11.893
Whole-core p-CMFD time (sec)	0	38.363	4.177	4.308	4.765	6.353	6.333	6.91
Total calculation time (sec)	19874.33	3891.21	471.662	464.529	455.566	199.425	189.887	181.254
Speedup	1	5.11	42.14	42.78	43.63	99.66	104.66	109.65
Percentage of transport sweep time in total calculation time	100.0	99.01	90.08	93.34	95.03	79.90	83.86	87.61

a: Gauss-Seidel +Power Iteration, b*: BiCGSTAB +Power Iteration, c*: BiCGSTAB +JFNK*

† : a single thread of a CPU (Intel i7-7700K)

5. Conclusions

Following and extending a previous report [2] on the coarse mesh acceleration methods and the two-level p-CMFD acceleration in the whole-core transport calculation, this paper presented a further speedup technique for p-CMFD acceleration in the whole-core transport calculation, that is also effective for optically thick coarse mesh cells (of assembly size). It is based on the two-level spatial coarse grid p-CMFD with global/local iterations in the low-order calculation. The test results show that we obtain fast convergence (even with large coarse-mesh cells), if we use a number of global/local iterations in TL(*N*)/p-CMFD with Krylov algorithms. This is owing to the availability of transport partial currents on the interface of two coarse mesh cells, allowing rebalance calculation via p-IMFD in each coarse-mesh problem (that can be performed in parallel and thus can reduce the local p-IMFD time further). More importantly, the most time-consuming transport sweep calculation footprint can be reduced further in a major way, if the transport sweep operations are performed characteristics by characteristics in parallel.

As a future work in another direction, the two-level p-CMFD method can be applied to the fast reactor analysis. Since the neutron mean free path is quite long in a fast reactor, the computational cells of super hexagonal- and rhombic-stencils could be considered (see Figure 7), following the procedures proposed in Ref. 20, based on the HIRE-theoretic multigroup transport equations with partial current discontinuity factors (PCDFs).

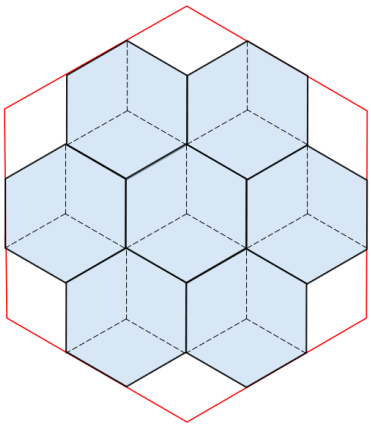

Figure 7. Super hexagonal/rhombic geometry representation for a fast reactor core.

Acknowledgements

The author expresses sincere thanks to Seungsu Yuk, YuGwon Jo, and Seongdong Jang of Korea Atomic Energy Research Institute, and Taesuk Oh of Korea Advanced Institute of Science and Technology, who provided valuable assistance during the preparation of this paper.

Disclosure Statement

No potential conflict of interest was reported by the author.

References

1. N. Z. CHO, Y. JO, and S. YUK, "A New Derivation of the Multigroup Transport Equations via Homogeneity and Isotropy Restoration Theory," Ann. Nucl. Energy, 110, 798 (2017); also presented in the Plenary Session at PHYTRA5 in Xian, China, May 10-11, 2021.
2. N. Z. CHO, "Comparative Review of Coarse-Mesh Acceleration Methods and the Two-Level p-CMFD Acceleration in the Whole-Core Transport Calculation," Atomic Energy Society of Japan, Reactor Physics Division Research Report No. 74, March 2022.
3. G. R. CEFUS and E. W. LARSEN, "Stability Analysis of Coarse-Mesh Rebalance," Nucl. Sci. Eng., 105, 31 (1990).
4. K. S. SMITH and J. D. RHODES III, "Full-Core, 2-D, LWR Core Calculations with CASMO-4E," Proc. PHYSOR 2002, Seoul, Korea, October 7–10, 2002, American Nuclear Society (2002) (CD-ROM).
5. N. Z. CHO, G. S. LEE, and C. J. PARK, "On a New Acceleration Method for 3D Whole-Core Transport Calculations," Annual Mtg. Atomic Energy Society of Japan, Sasebo, Japan, March 27–29, 2003, Atomic Energy Society of Japan (2003).
6. N. Z. CHO, G. S. LEE, and C. J. PARK, "Partial Current-Based CMFD Acceleration of the 2D/1D Fusion Method for 3D Whole-Core Transport Calculations," Trans. Am. Nucl. Soc., 88, 594 (2003).
7. N. Z. CHO, "The Partial Current-Based CMFD (p-CMFD) Method Revisited," Trans. Kor. Nucl. Soc., Gyeongju, Korea, October 25–26, 2012, Korean Nuclear Society (2012).
8. N. Z. CHO and C. J. PARK, "A Comparison of Coarse Mesh Rebalance and Coarse Mesh Finite Difference Accelerations for the Neutron Transport Calculations," Proc. M&C 2003, Gatlinburg, Tennessee, April 6–11, 2003, American Nuclear Society (2003); see also KAIST internal report NURAPT-2002-02, (with addendum on p-CMFD); https://github.com/nzcho/Nurapt-Archives/blob/master/NurapT2002_2rev2.pdf
9. A. YAMAMOTO, "Generalized Coarse-Mesh Rebalance Method for Acceleration of Neutron Transport Calculations," Nucl. Sci. Eng., 151, 274 (2005).
10. S. YUK and N. Z. CHO, "Two-Level Convergence Speedup Schemes for p-CMFD Acceleration in Neutron Transport Calculation," Nucl. Sci. Eng., 188, 1 (2017); and Corrigendum, 188, 303 (2017).
11. N. Z. CHO, "An Overview of p-CMFD Acceleration and Its Applications to Reactor Physics Transport Calculation," Trans. Am. Nucl. Soc., 117, 1247-1250 (2017); and also "Incorporation of Temperature Feedback Effect in HIRE-Theoretic Multigroup Transport Equations," presented at Osaka University, May 16, 2018.
12. N. Z. CHO, "The Roles of Transport Partial Current Information in Two-Level p-CMFD Acceleration in the Whole-Core Transport Calculation," Trans. Am. Nucl. Soc., 121, 1323-1326 (2019).
13. N. Z. CHO, "Krylov Subspace Wraps around the Two-Level p-CMFD Acceleration in the Whole-Core Transport Calculation," Trans. Am. Nucl. Soc., 123, 1327-1330 (2020).

14. D. WANG and S. XIAO, "A Linear Prolongation Approach to Stabilizing CMFD," Nucl. Sci. Eng., 190, 45 (2018).
15. A. ZHU, M. JARRETT, Y. XU, B. KOCHUNAS, E. W. LARSEN, and T. DOWNAR, "An Optimally Diffusive Coarse Mesh Finite Difference Method to Accelerate Neutron Transport Calculations," Ann. Nucl. Energy, 95, 116 (2016).
16. Y. SAAD, "Iterative Methods for Sparse Linear Systems," SIAM, 2003, pp. 231-234 (BiCGSTAB algorithm for Krylov method).
17. H. PARK, D. A. KNOLL, and C. K. NEWMAN, "Nonlinear Acceleration of Transport Criticality Problems," Nucl. Sci, Eng., 172, 52 (2012).
18. M. A. SMITH, E. E. LEWIS, and B.-C. NA, "Benchmark on Deterministic Transport Calculations Without Spatial Homogenization: A 2-D/3-D MOX Fuel Assembly 3-D Benchmark," NEA/NSC/DOC(2003)16, Organisation for Economic Co-operation and Development, Nuclear Energy Agency (2003).
19. N. Z. CHO, "An Enlarged 2-D OECD/NEA Benchmark Problem and Two-Level p-CMFD Solutions," Korea Advanced Institute of Science and Technology, June 2020; https://github.com/nzcho/Nurapt-Archives/blob/master/NZCho_ANS_W2020_Addendum.4.pdf
20. N. Z. CHO, "A Proposed New Framework for Reactor Physics Analysis with Transport Calculation," Trans. Kor. Nucl. Soc., Yeosu, Korea, October 24-26, 2018, Korean Nuclear Society (2018); https://www.kns.org/files/pre_paper/40/18A-132 조남진 I.pdf